Biomaterials Science

ROYAL SOCIETY OF CHEMISTRY

PAPER

View Article Online
View Journal | View Issue

Cite this: *Biomater. Sci.*, 2025, **13**, 5825

Non-destructive approaches for retrieving T-cells from fibrous scaffolds for therapeutic applications

Jaydeep Das, [a] Neil R. Cameron *[b,c,d] and Prakriti Tayalia *[e]

Flasks and plates have traditionally been used to culture cells required for cell-based therapies. Recent success of adoptive T-cell transfer therapy (ACT) for various pathological conditions warrants development of more physiologically relevant *ex vivo* cell culture platforms. Electrospun (Espun) scaffolds hold promise for culturing cells by mimicking features of extracellular matrix (ECM). However, unlike traditional 2D culture, recovering cells from these fibrous scaffolds is challenging and poses a critical roadblock in their development as cell culture platforms. We used electrospun matrices to culture Jurkat T-cells and observed that the cells remain entrapped in these matrices, facilitating their growth and clustering, which are the key phenomena for their activation and expansion, especially in the context of adoptive cell therapy. Yet, their retrieval using the pipette-aided gentle aspiration method proved difficult. This challenge was amplified with stimulating (anti-CD3 antibody-coated) substrates. Our study compared different recovery strategies using enzymatic agents (Accutase and TrypLE) and non-enzymatic manual flushing to determine the most effective method. A comparable cell yield was obtained and the viability of recovered cells was found to be unaffected for all the methods tested. However, the unstimulated substrate had a significantly higher cell recovery than its stimulated counterpart. Further investigation revealed that cells recovered from scaffolds after enzymatic treatment with Accutase had better proliferation and clustering ability when compared with those cultured on 2D substrates. The insights from this study may be critical in generating clinical-grade T-cells *ex vivo* for immunotherapeutic applications.

Received 10th June 2025,
Accepted 15th August 2025

DOI: 10.1039/d5bm00877h

rsc.li/biomaterials-science

1 Introduction

Physiologically relevant matrices or scaffolds are crucial for tissue engineering and immunotherapeutic applications, serving as 3D cell culture platforms.[1,2] Among these, electrospun (Espun) scaffolds have gained significant attention due to their scalability, simplicity, ease of functionalization, and the wide variety of polymers that can be used.[3,4] Researchers are increasingly exploring the potential of electrospun fibres for generating high-quality T-cells in T-cell transfer therapy.[5,6] This interest is driven by the fibres' ability to closely mimic the structural and topological features of the extracellular matrix in secondary lymphoid organs.[7,8]

Electrospun polycaprolactone (PCL) fibres are particularly promising due to their large surface area, FDA approval, and biocompatibility.[4] While these fibres have been successful in various tissue engineering applications, their use in immune cell culture,[9] specifically for T-cell expansion, is relatively new.[5,6] Contrary to the traditional belief that T cells are entirely suspended in nature and do not adhere to surfaces, a significant body of literature indicates that T cells actively engage with the substrates on which they migrate. They can also alter their morphology and functions in response to the ligands and complex topographies present on the culture substrate.[10,11] For example, in secondary lymphoid organs, hosts have fibrous reticular networks comprising extracellular matrix components.[12] In recent developments, researchers have begun to replicate densely packed fibrous reticular networks through the use of electrospun scaffolds.[7]

A major challenge with these matrix systems is retrieval of cultured T-cells from the intricate mesh network of fibres. In a recent study, electrospun scaffolds coated with dendritic cell membranes were used to activate T lymphocytes. Although this method showed promise, the researchers encountered difficulties related to inefficient cell harvesting and incomplete fibre removal.[6] Partial removal of fibres increases the chances

[a]*IITB-Monash Research Academy, Powai, Mumbai, Maharashtra 400076, India*
[b]*Department of Materials Science and Engineering, Monash University, 20 Research Way, Clayton, Victoria, 3800, Australia. E-mail: neil.cameron@monash.edu*
[c]*School of Engineering, Warwick University, Coventry CV4 7AL, UK*
[d]*Nanotechnology & Catalysis Research Centre, Institute for Advanced Studies (IAS), Universiti Malaya, 50603 Kuala Lumpur, Malaysia*
[e]*Department of Biosciences and Bioengineering, Indian Institute of Technology Bombay, Powai, Mumbai, Maharashtra 400076, India. E-mail: prakriti@iitb.ac.in*

of adverse response of cells *in vivo* due to overstimulation leading to host cell death. Moreover, the remnant impurities can lead to disruption of various cell manufacturing stages of ACT. Our study seeks to address these challenges.

In this study, we prepared electrospun scaffolds as substrates for *ex vivo* T cell culture and expansion. Our initial goal was to determine whether Jurkat T-cells could be cultured on both unmodified and antibody-coated scaffolds while maintaining their viability. We also aimed to investigate whether these cells could be effectively removed from both types of scaffolds using various cell recovery methods. We studied three recovery methods, wherein the first two methods involve use of commercially available enzymatic cell recovery agents, Accutase™ and Trypsin (TrypLE™), while the third method is non-enzymatic and involves pipette-aided flushing and aspiration. These methods were compared in terms of cell yield and functionality for downstream applications. The information obtained from this study will be instrumental in devising the ideal protocol for retrieving T cells from scaffolds.

2 Experimental

2.1 Fabrication of electrospun scaffolds

To prepare for electrospinning, PCL (M_n = 80 000; Sigma Aldrich) pellets were dissolved in acetone and stirred at 65 °C to form a 10% (w/v) solution. The polymer solution was loaded into syringes fixed with blunt-ended 18 G needles (BD Biosciences) and was electrospun in a closed chamber electrospinning unit (SUPER ES-3, E-spin Nanotech). The spinning process involved using an electrostatic potential of 18 kV and an aluminium foil-covered rotating (at a speed ranging from 1200–1500 rpm) drum collector at a distance of 9.5 cm from the needle. The feeding rate was kept constant 1 μl s^{-1} using a syringe pump. The fibrous mat deposited on the collector was removed, and disks of desired diameters were punched using a clean biopsy punch.

2.2 Pre-treatment of scaffolds for cell culture

16 mm disks of electrospun PCL scaffolds were soaked in 80% ethanol for 30 min, followed by thorough rinsing with 1× PBS thrice (the last wash includes overnight soaking in 1× PBS). Next, the scaffolds were UV sterilized on both sides for 30 min (each side) and allowed to dry completely inside a Class II biosafety cabinet. The disks were then placed carefully in a sterile non-tissue culture treated 24-well plate using a pair of sterile forceps or stored for future use. For antibody coated scaffolds, one day prior to cell seeding, the disks were kept in 24-well plates and soaked overnight at 4 °C in T cell activating anti-hu-CD3 (BioLegend – Cat No. 317301) (0.5 μg ml^{-1}) antibody prepared in ice-cold PBS at a dilution of 1 : 400. Excess antibody was washed and the co-stimulating anti-hu-CD28 (BioLegend Cat No. 302901) antibody (0.5 μg ml^{-1}) was added to the media at the time cell seeding.

2.3 Characterization of scaffold morphology

Scanning electron microscopy. Scanning electron microscopy (SEM) was conducted to evaluate the pore size and fibre diameter of the scaffolds. 10 mm discs of electrospun scaffolds were affixed to clean metallic stubs with adhesive conductive carbon tape. The scaffolds were then coated with gold using a sputter coater (Quorum Q150R Plus) for 2 minutes. After coating, the gold-coated scaffolds were loaded into a Scanning Electron Microscope (Phenom Pro), where images were acquired at various magnifications.

To estimate the pore size, perimeters of visible pores were measured at four random locations on the fibrous scaffold using Fiji (ImageJ) software, with 20 pores chosen at each location. Fibre circumference was quantified from the SEM images using the DiameterJ plugin implemented in ImageJ. Next, the radius was calculated using the equation $C = 2\pi r$, where C is the perimeter or circumference of the pore and r is the radius. The diameter (D) was then determined as $D = 2r$. Additionally, fibre diameter distribution was calculated from SEM images taken at four random sites with 25 fibre measurements collected per site.

Fluorescence microscopy. A solution of Sudan Black (SB) at a concentration of 0.1% was prepared by dissolving SB powder in 70% (v/v) ethanol and was kept on a rocker to obtain a homogenous solution. The solution was then syringe-filtered using a 0.2 μm filter. The scaffold samples were immersed in SB solution overnight at 4 °C. Following the staining process, the samples were rinsed three times with 1× phosphate-buffered saline (1× PBS) and exposed to UV light for sterilization. Sterile electrospun scaffolds were placed in the wells of a 24-well plate on a rocking platform and soaked overnight at 4 °C in goat anti-rabbit IgG AF488 antibody (Invitrogen), diluted 1 : 400 in ice-cold 1× PBS. This process allowed for maximum adsorption of the antibody onto the matrix. After soaking, the scaffolds were gently washed with 1× PBS to remove any unbound antibody. Next, the scaffolds were transferred to a clean 35 mm glass bottomed confocal dish and imaged using an Olympus FV3000 confocal microscope.

2.4 Cell culture

Jurkat cells, which are immortalized human $CD4^+$ T cells, were obtained from the American Type Culture Collection (ATCC) and used as model cell lines. The cells were cultured according to the protocols established by ATCC in RPMI-1640 medium (with or without phenol red) supplemented with 2 mM L-glutamine and 10% (v/v) fetal bovine serum (FBS), referred to as complete growth medium. Cultures were maintained under standard conditions of 37 °C, 5% carbon dioxide, and 95% relative humidity. The cell concentration was kept between 1×10^5 and 1×10^6 viable cells per mL. Every two days, the spent medium was removed, and fresh medium was added to the culture. Cell numbers and viability were assessed using the Trypan blue dye exclusion method and counted manually with a hemocytometer.

Cell seeding on scaffolds. On the day of cell seeding, 0.5×10^6 Jurkat cells were stained with Hoechst (1 μg ml^{-1}) prepared in 1× PBS. Depending upon the scaffold experimental group, the co-stimulating anti-CD28 antibody was added (or not) to the growth media used for resuspending the cell pellet and seeding the cells onto the scaffold. Fresh media was added every two days for the duration of long-term cell culture.

2.5 Cell recovery from 2D and 3D substrates

0.5×10^6 Jurkat cells were seeded either per well onto a 24-well, non-tissue culture-treated plate (2D) and or onto each 15 mm disk of electrospun scaffolds (3D). After 3 days of culture, the cells were either gently aspirated from 2D wells. For cell recovery from scaffolds, various cell recovery methods were employed as described later. Brightfield microscopy was used to visualize the cells before and after aspiration on 2D wells while pre- and post-recovery fluorescence confocal microscopy was employed to visualize the cells on the scaffolds. Cell counting and assessment of cell viability were conducted using the Trypan blue dye exclusion method.

Cell recovery techniques. Three strategies were used to recover T-cells from the scaffolds. The first two strategies involved commercially available enzymatic recovery agents, Accutase™ and TrypLE™, while the third strategy utilized a pipette-aided scaffold flushing and aspiration method. Initially, 0.5×10^6 Jurkat cells were seeded onto the 2D and unmodified antibody-coated scaffolds, as described previously. The cells were allowed to grow for up to 7 days. At designated time points, the cell-laden scaffolds were carefully transferred to new 12-well plates that were pre-filled with undiluted cell dissociation reagents. The scaffolds were immersed in these reagents for 5 minutes at 37 °C. After incubation, the lytic activity of the reagents was neutralized by adding serum-supplemented growth media at twice the volume of the enzyme solution. Our preliminary qualitative microscopy-based assessment, conducted using Jurkat cells and splenocytes, has shown that exposing T lymphocytes to enzymatic cell dissociation agents for more than 10 minutes compromises cell viability. Therefore, we decided to use a 5-minute exposure time, as recommended in the product information sheet (Catalog No. A6946 – Accutase, Sigma-Aldrich and TrypLE-Invitrogen). Entire scaffold was rinsed thoroughly with complete growth media for about 15 to 20 times. Subsequently, cells were collected from both the primary well initially containing the scaffold and the new well containing the rinsed media. The cell suspension was pooled and centrifuged, while the cells were counted using the Trypan blue dye exclusion method and a manual hemocytometer. In the third strategy, cell recovery was done by vigorously flushing the scaffolds using a pipette before aspiration.

2.6 Assessment of cell viability

The viability of recovered cells was measured using the Trypan blue dye exclusion method and a manual hemocytometer. Calcein AM and Propidium Iodide (PI) were used as cell viability indicators for fluorescence microscopic assessment. The assay was performed using 2 μM Calcein AM (C3100MP, Invitrogen) and 1.5 μM PI (P3566, Invitrogen) in phenol red-free growth medium. First, the cells were washed twice with phenol red-free growth medium. Next, 2 μM Calcein AM was added to the cell suspension and incubated at room temperature for 30 minutes with protection from light. After incubation, the cells were washed and stained with 1.5 μM PI, followed by a 5-minute incubation at room temperature with protection from light. The cells were then washed twice and loaded onto a clean 35 mm glass bottomed confocal dish. Image acquisition was performed using an Olympus FV3000 confocal microscope.

The viability of Hoechst-stained cells adherent to the scaffolds pre- and post-recovery, was assessed by soaking them in Calcein AM stain for 45 minutes to allow for better dye penetration. The scaffolds were then washed with pre-warmed 1× PBS or phenol red-free RPMI 1640. Subsequently, the scaffolds were transferred to confocal dishes and imaged using the confocal microscope.

2.7 Assessment of cell proliferation

The proliferation of recovered cells was assessed using the carboxyfluorescein succinimidyl ester (CFSE) dye dilution method, following the manufacturer's protocol. In brief, 0.5×10^6 Jurkat cells were seeded on 2D non-adherent 24-well plates, unmodified surfaces and functionalized electrospun scaffolds with T cell-stimulating antibodies (as previously described) and cultured for 72 hours. After this period, they were retrieved from the scaffolds either using manual flushing alone or followed by treatment with TrypLE and Accutase. The cells were then centrifuged, and the spent media was discarded. The cell pellet was resuspended in a CFSE dye staining solution (5 μM), prepared in sterile 1× PBS and incubated for 20 minutes at 37 °C with protection from light. Following incubation, any remaining free dye was removed by adding a volume of complete medium that was five times greater than the original staining volume. The cells were centrifuged again, and the supernatant was discarded. The cells were then reseeded onto non-tissue culture-treated 24-well plates that had been pre-coated with anti-CD3 antibody. Co-stimulation was provided by adding soluble anti-CD3 antibody at the time of seeding. The cells were then cultured for a week to monitor CFSE dye dilution and cell proliferation was measured on days 3 and 7 post cell-seeding. At each time point, the cells were collected from the respective wells, washed three times with ice-cold 1× PBS, and fixed with 1% PFA. Finally, the cells were analyzed using a Cytoflex Flow Cytometer (Beckman Coulter).

2.8 Statistical analysis

All data are presented as mean ± standard deviation (s.d.), unless otherwise stated. Assays were conducted in triplicate, unless otherwise specified. Statistical analysis was carried out using GraphPad Prism 10 software (version 10.2.3), applying one-way analysis of variance (ANOVA) followed by Tukey's *post hoc* test or Dunnett's multiple comparison test, as indicated in the figure captions. For specific experiments, results were analyzed using two-way ANOVA with Tukey's post-hoc tests, as indicated in the figure captions. In all cases, a p-value of less than 0.05 was deemed statistically significant.

3 Results

3.1 Architecture of electrospun scaffolds facilitates cell-trapping

The fibrous electrospun scaffolds were optimized for various process parameters (Table S1) to eliminate beading seen in the fibres produced initially when examined under a brightfield microscope. The mats spun by electrospinning the entire PCL polymer solution were punched into scaffolds of desired sizes and subjected to physical characterization using scanning electron microscopy (SEM) and fluorescence microscopy (Fig. 1a, b and S1). The average pore size was found to be 9.0 ± 1.0 μm and the fibre diameter was 2.0 ± 0.9 μm (Fig. 1c and d). The range of fibre diameters obtained in this study is similar to that of the artificial antigen-presenting cell (APC) particles found to be effective in activating primary T-cells reported earlier.[13] This pore size range allowed the Jurkat cells, which are about 10–16 μm in size,[14] to fit into the interconnected mesh network, thereby providing an increased opportunity for cell–cell and cell–material interactions (Fig. 1e and f).

Immune cells are sensitive to the architecture of the substrates on which they are cultured and expanded.[10,11,15,16] Furthermore, immune cells are known to probe their environment, sensing mechanical stimuli through their mechanosensors, which can temporarily anchor them to a compatible substrate.[17,18] This behaviour underscores the relevance of the architecture of scaffold on cell–material interactions and highlights the importance of effectively removing the cells from these

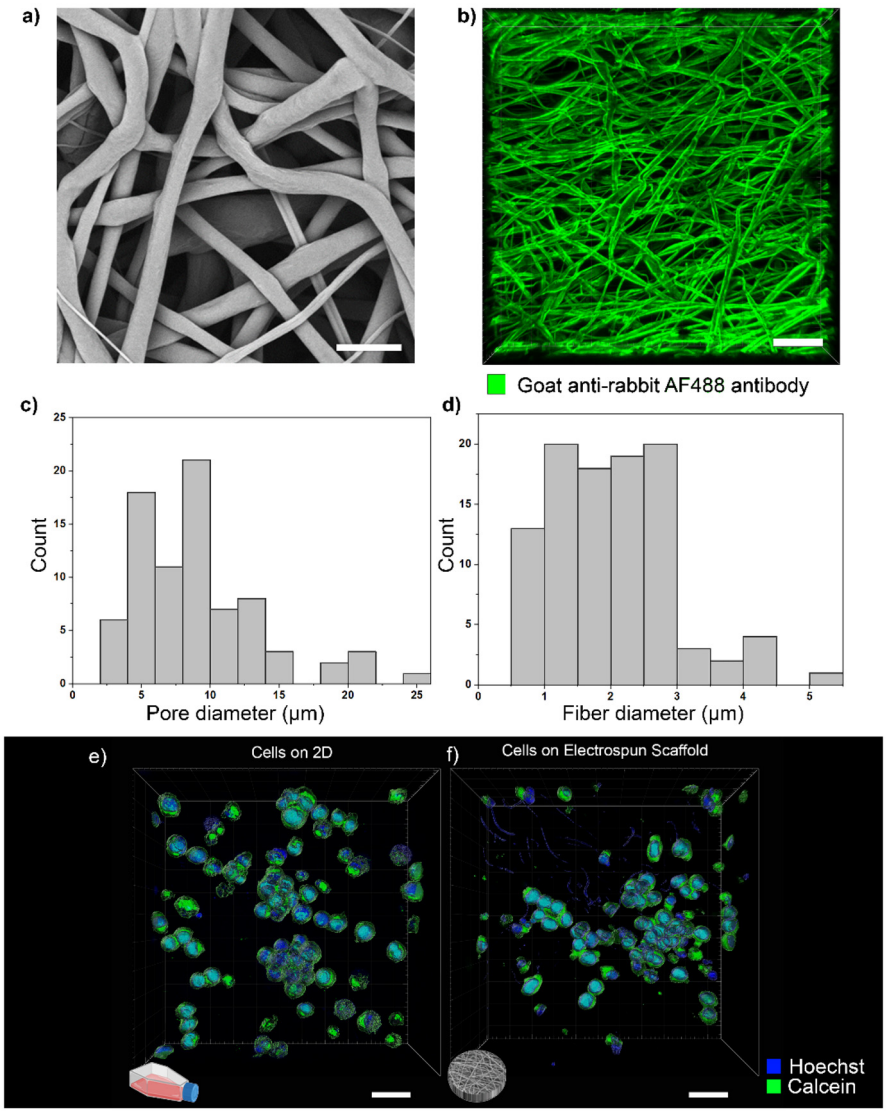

Fig. 1 Physical and biological characterisation of electrospun scaffolds. (a) Scanning electron micrograph of electrospun (Espun) PCL scaffold; (b) confocal images of an antibody (Goat anti-Rabbit IgG AF488)-coated electrospun scaffold showing intricate mesh-like features; (c) pore diameter and (d) fibre diameter distribution determined from SEM images using Image J software; 3D rendered top view of Jurkat cells on a (e) 2D and an (f) electrospun scaffold stained with nuclear dye Hoechst and cytoplasmic dye Calcein AM. For 3D rendering, the *z*-stack of confocal images were processed using Imaris Software (ver. 10.1.1); scale: (a) 10 μm, (b), (e) and (f) 30 μm.

scaffolds for downstream applications. To compare cell recovery from 2D and 3D substrates, Jurkat cells were cultured on conventional non-tissue culture-treated plates (2D) and on Espun scaffolds (3D) for 72 hours. At the study endpoint, pipette-aided aspiration and varying intensity of mechanical flushing was used to recover cells. Images of substrates were captured before and after pipette-aided aspiration to compare the extent of cell recovery. Cells prestained with fluorescently labelled nuclear dye, Hoechst, enabled their visualization within the electrospun scaffolds to assess the extent of recovery pre- and post-aspiration.

Unlike 2D substrates, the 3D scaffolds present a greater challenge to cell removal (Fig. 2a–c). Jurkat T-cells, which are suspension cells, exhibit partial adherence to the 3D substrates, further complicating their recovery from the scaffolds (Fig. 2d–f). To investigate the relative position of cells within the 3D fibrillar matrix, the electrospun fibres were also labelled with a secondary antibody (goat anti-rabbit AF488). Confocal microscopy images revealed that the cells resistant to detachment were mostly located at the junctions of crossing fibres (Fig. 2g and h), which partially explains the resistance offered by 3D matrices to cell retrieval. The interweaved junctional regions provide more contact points to T cells to form effective cell–cell and cell–material interactions. Also, the strut like features of the electrospun fibres act as a mesh and at the

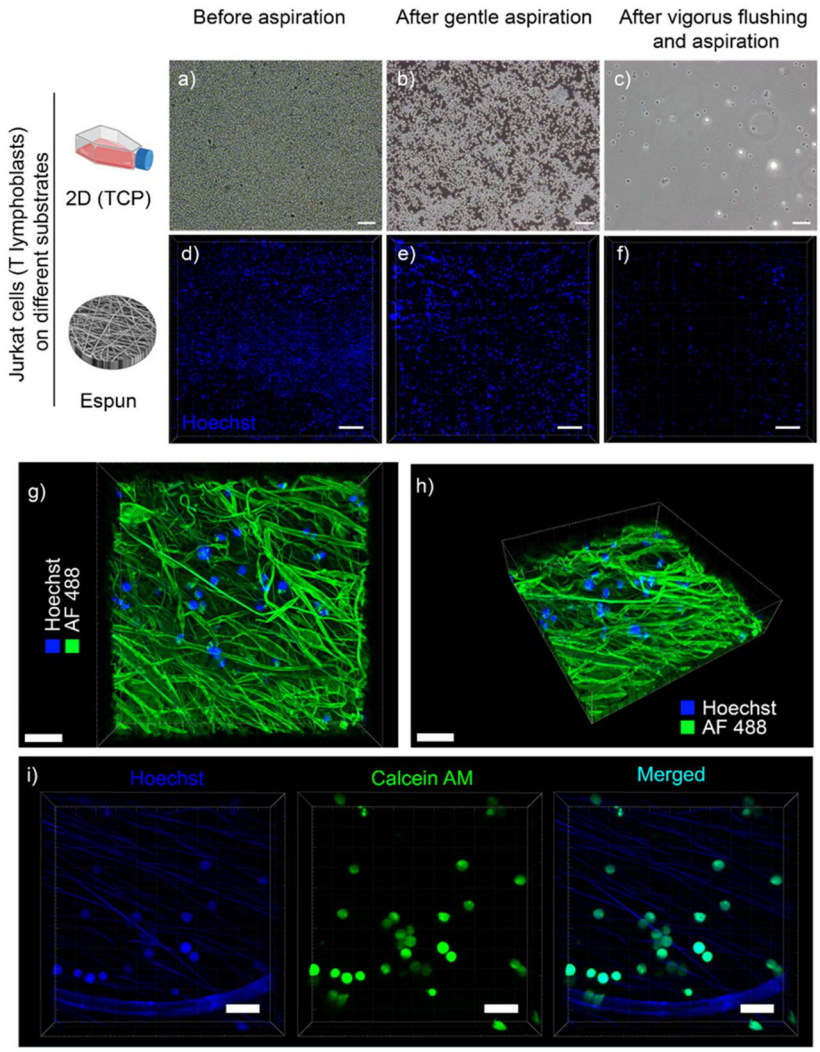

Fig. 2 Jurkat cells remain firmly adhered to the fibrous scaffold. (a–c) Brightfield images of cells on 2D (non-adherent tissue culture plasticware, TCP) and (d–f) confocal images of cells in electrospun scaffold on day 3 after subjecting them to pipette aided cell aspiration. Jurkat cells as seen in a non-adherent 24 well plate (a) undisturbed (b) after gentle aspiration and (c) after vigorous flushing followed by aspiration. To visualize cells on opaque Espun scaffolds, cell nuclei were stained with Hoechst (Blue) and imaged by confocal microscopy. *Z* stack images were visualized using Imaris Viewer (ver. 10.1.1). Jurkat cells on Espun scaffold as visualized (d) prior to aspiration and remaining attached to scaffold (e) after gentle aspiration and (f) after vigorous aspiration. The Espun scaffolds were stained with Sudan Black B to minimize autofluorescence. (g and h) 3D rendered view of Jurkat cells remaining on Espun scaffold post vigorous aspiration. (g) top view and (h) side view of the cell-laden scaffold; (i) confocal image showing Jurkat cells remaining on the scaffold (stained blue with Hoechst) and that are viable (stained green with Calcein AM). Scale: (a–c) 250 μm, (d–f) 150 μm, (g and i) 30 μm and (h) 40 μm.

intersection of fibres, the pores further decrease in size, allowing cell entrapment. Moreover, the remnant scaffold bound cells stay viable (Fig. 2i).

3.2 Cell recovery from electrospun scaffolds is comparable across various recovery techniques

For downstream applications, cells need to be removed from the scaffold, through a process that does not affect cell health. To our knowledge, there is minimal information on effective recovery of T-cells from scaffolds correlating it to their health and function. Here, various parameters such as the number of cells recovered, their proliferative and functional properties were compared across the three cell recovery methods to identify the most optimum method. Further, to check if cell detachment was more challenging in the presence of T-cell-stimulating agonistic antibodies (anti-CD3 and anti-CD28), Jurkat-cells were seeded on both unmodified and antibody-functionalized 2D substrates as well as scaffolds and cultured for 72 hours. Cell recovery using two of the most widely used cell dissociation agents, namely TrypLE and Accutase[19] and a manual pipette aided flushing method were compared (Fig. 3a). TrypLE is a mild enzymatic cell dissociation agent used for a broad range of adherent cell types while Accutase is another mild enzymatic cell detachment agent commonly used for various downstream applications.

T-cells are reported to be mechanosensitive, with mechanotransduction occurring *via* mechanosensors, some of which are located on cell surface and interact with the matrix.[17,18] In this study, the enzymatic agents were cautiously used to avoid damaging crucial cell surface receptors essential for T-cell activation and proliferation.[19] After cell recovery, the pooled cell suspensions from primary and secondary wells (as mentioned earlier), where the scaffold was transferred for dissociation were counted. As expected, recovering cells from the antibody-functionalized scaffolds was more challenging than that from the unmodified ones due to the influence of strong cell-scaffold interactions in functionalized scaffolds (Fig. 3b). The graph in Fig. 3b shows the absolute count of the viable cells which were recovered from the native and antibody coated scaffolds using various methods of cell recovery. The percentage cell recovery from the antibody coated substrates (Ab_2D_MF, Ab_TrypLE and Ab_Accutase) was comparable across the various recovery methods used which was around 47%, 31%, 32%, 33% respectively. Moreover percentage cell recovery from the uncoated substrates (MF, TrypLE, and Accutase) was around 88%, 89%, and 75% respectively. In terms of % viability of the recovered cells. Accutase-mediated recovery resulted in the smallest difference in viability between cells recovered from uncoated and antibody-coated scaffolds, indicating its gentle and consistent performance across substrate types (Fig. S8). Cell recovery was comparable across all test groups, with no significant difference observed (Fig. S2b and S2d). Cell viability remained largely unaffected by the recovery method (Fig. 3c and d). However, there was an increase in the dead cell population when cells were retrieved from the antibody-functionalized scaffolds (Fig. S2e). This increase was likely due to the overstimulation of cells by the activating ligands presented by the scaffolds, which may have led to activation-induced cell death.[20,21] These observations underscore the importance of transient stimulation of T-cells with activating antibodies to match physiological stimulation, which may help maintain cell viability for downstream applications.

3.3 Recovery methods do not affect the proliferation of cells

The goal of recovering immune cells is to use them for therapeutic purposes.[22,23] However, depending upon the method of recovery, cells are subjected to shear forces or enzymatic treatment, which may adversely affect cell health. To test this, the proliferative capacity and clustering ability of the recovered cells were assessed since healthy and functionally active T-cells are known to form large cell clusters.[13,24] Cells seeded on 2D surfaces, unmodified scaffolds, and antibody-coated Espun scaffolds were recovered after 3 days of culture. They were further stained with CFSE (cell proliferation) dye and cultured on stimulating (anti-CD3 antibody coated) 2D substrates until Day 7. Cells recovered from various substrates exhibited minimal proliferation on Day 3, indicated by only a slight left shift of the CFSE fluorescence intensity peak when compared to the control peak on Day 0 (Fig. 4a). Since proliferating T-cells were indicated by reduced fluorescence intensity due to dye dilution, it was found that the antibody-coated scaffolds led to more proliferation of cells than the unmodified scaffolds by Day 3, as shown in Fig. 4a. However, by Day 7, the number of proliferating cells recovered from antibody-coated scaffolds were significantly higher than those from the unmodified scaffolds (Fig. 4a and Fig. S3a). This significant increase in proliferating cells from Day 3 to Day 7 suggests that the recovered cells retained their proliferative capacity and that the recovery method had minimal impact on cell health and functional integrity. Further, reduction in mean fluorescence intensity (MFI) of recovered cells, which also suggests cell proliferation and dye distribution among daughter cells, is indicated by CFSE dye dilution. A reduction in the MFI values from Day 3 to Day 7, irrespective of the test groups and the scaffold type used again implies that the recovered cells retain their proliferative capacity (Fig. 4b and c). Furthermore, the MFI was found to be significantly reduced for cells recovered using Accutase from the stimulating scaffolds compared to the conventional antibody-functionalized 2D control on Days 3 and 7 (Fig. 4c.1 and c.2). Cell size or spreading is another parameter that has been studied as an indicator of metabolically active cells. Here, cell spreading post-recovery was analyzed to understand the impact of recovery methods on cell health (Fig. S4). Further, activated and potent T-cells are known to spread on a substrate in response to TCR stimulation.[25,26] Healthy cells with active cellular esterases are known to cause rapid hydrolysis of the non-fluorescent and membrane-permeable Calcein AM, leading to the release of brightly fluorescent Calcein within the cell cytoplasm. This cleaved product is thus seen as an intense green fluorescing signal in live cells, where the signal intensity corresponds to cell health. In this study, the

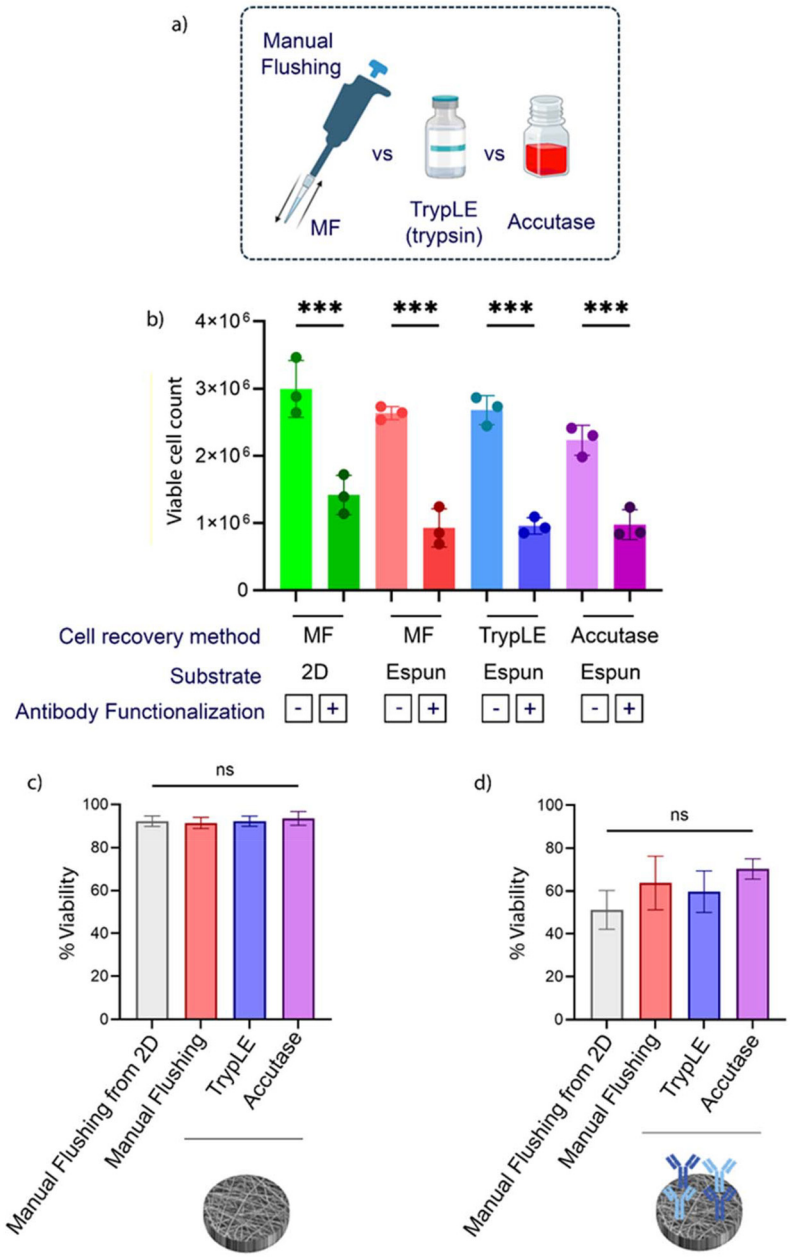

Fig. 3 T-cell recovery from unmodified and antibody-coated scaffolds. (a) Schematic showing the various cell recovery methods adopted for Jurkat cell removal from fibrous scaffolds. (b) Graph showing the total viable cells recovered from unmodified and antibody-coated scaffolds using the various recovery methods. Graphs comparing the cell viability using the different recovery methods from (c) unmodified and (d) antibody-coated electrospun matrices. Data in (b, c, and d) represent mean ± s.d. where $n = 3$ and analysed using one-way ANOVA, followed by Tukey's *post hoc* test in GraphPad Prism software (ver.10.0), $*p < 0.05$, $**p < 0.01$, $***p < 0.001$ ns: not significant.

cells recovered using Accutase showed a much more intense green signal compared to the other recovery methods (Fig. S5). This indicates that Accutase-based recovery does not compromise the health of T-cells.

3.4 Jurkat cells retain their clustering ability post-recovery

Brightfield images captured on Day 3 post-culture showed that the recovered cells retained their ability to cluster, which is essential for cell proliferation. Maximum clusters were observed for cells recovered from antibody-coated electrospun scaffolds, which make them preferred for therapeutic use, followed by unmodified scaffolds and the widely used 2D modified substrates (Fig. 5). The above data clearly shows that the Accutase-based cell recovery could be an ideal method for T-cell recovery from fibrous scaffolds. Recovery of T-cells from electrospun scaffolds is an underexplored area and the potential of these substrates to expand therapeutic-grade T-cells for pre-clinical and clinical research requires further investigation.

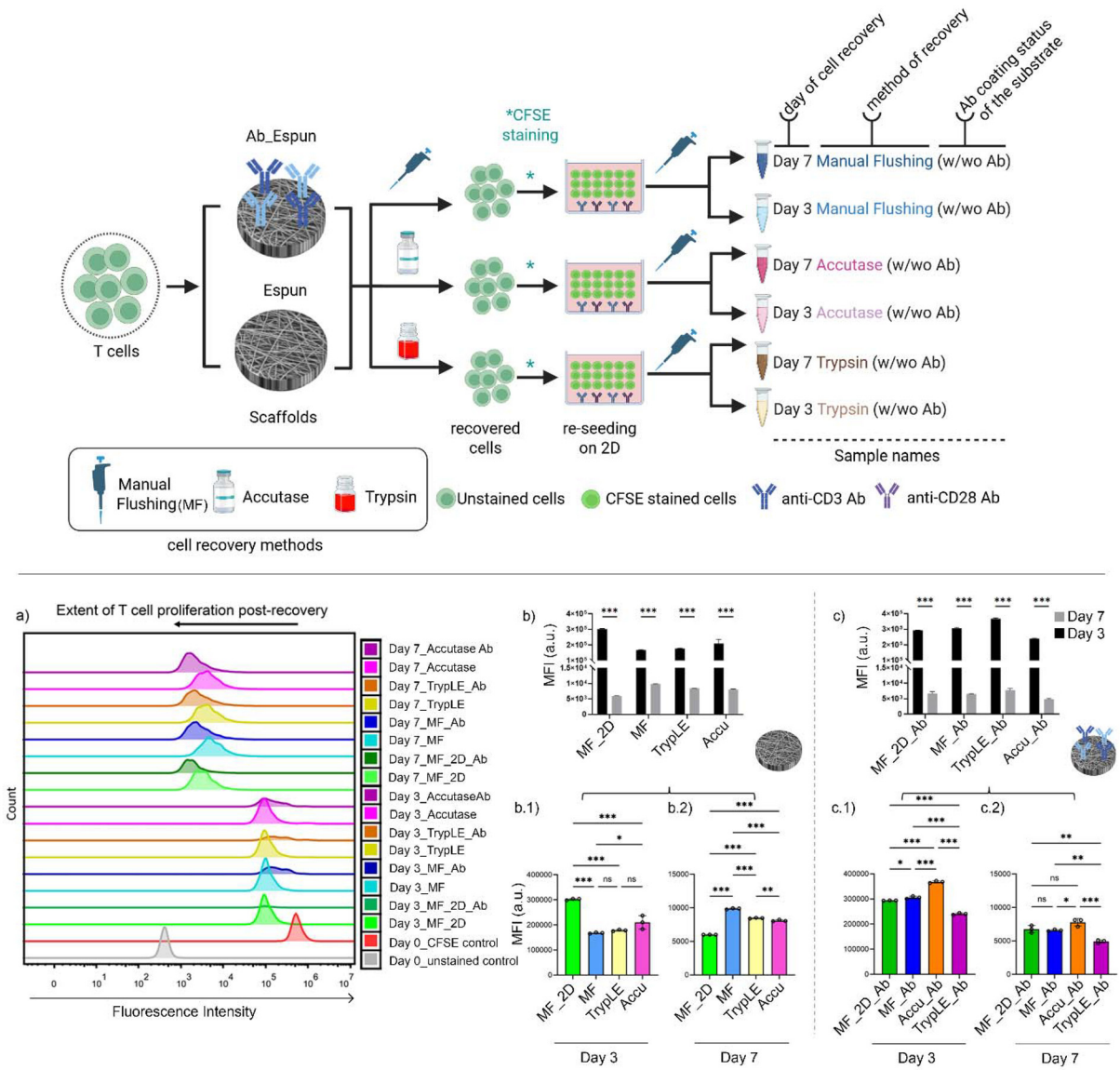

Fig. 4 T-cells recovered from unmodified and antibody-coated substrate retain their ability to proliferate. Top-schematics showing the experimental setup to compare the effect of cell recovery method on cell proliferation. (a) Histograms showing the extent of proliferation of recovered cells on Day 3 and Day 7 as indicated by the reduction in the fluorescence intensity due to CFSE dye dilution. Comparison of mean fluorescence intensity (MFI) of the cells recovered from (b) unmodified and (c) antibody-coated scaffolds that were allowed to grow on 2D until Day 3 and Day 7. MFI values of the recovered cells from unmodified scaffolds on b.1) Day 3 and and b.2) Day 7, and from antibody-coated scaffolds on c.1) Day 3 and and c.2) Day 7, respectively. Data (b, c, b.1, b.2, c.1 and c.2) represent mean ± s.d.; data in b, c was analyzed using two way ANOVA and in b.1, b.2, c.1, c.2 using one-way ANOVA using with Tukey's *post-hoc* test; $*p < 0.05$, $**p < 0.01$, $***p < 0.001$. $n = 3$ for triplicate experiments.

Studies have shown that Accutase recovers more macrophages from Espun scaffolds than EDTA, Trypsin, or PromoCell Macrophage Detachment Solution (PMDS), likely due to easier detachment from thin electrospun fibres. While recovery methods differ, Accutase has proven more effective in yielding healthy cells compared to other techniques.[27] Further, cell yield also varies between 2D and 3D substrates, especially for adherent cells like macrophages. However, studies comparing the yield of suspension cells, such as T-cells, will provide deeper insights into their performance and utility.

4 Discussion

Over the last decade, various substrates have been used as T-cell activation and expansion platforms. These are either elastomers, hydrogels, or extracellular matrix mimetic scaffolds. ECM mimetic fibrous scaffolds have recently been used as *ex vivo* T cell activating platforms.[5,6] In this study, the utility of electrospun fibrous platform was explored for adoptive T-cell transfer therapy. Currently, information regarding the cell harvest-

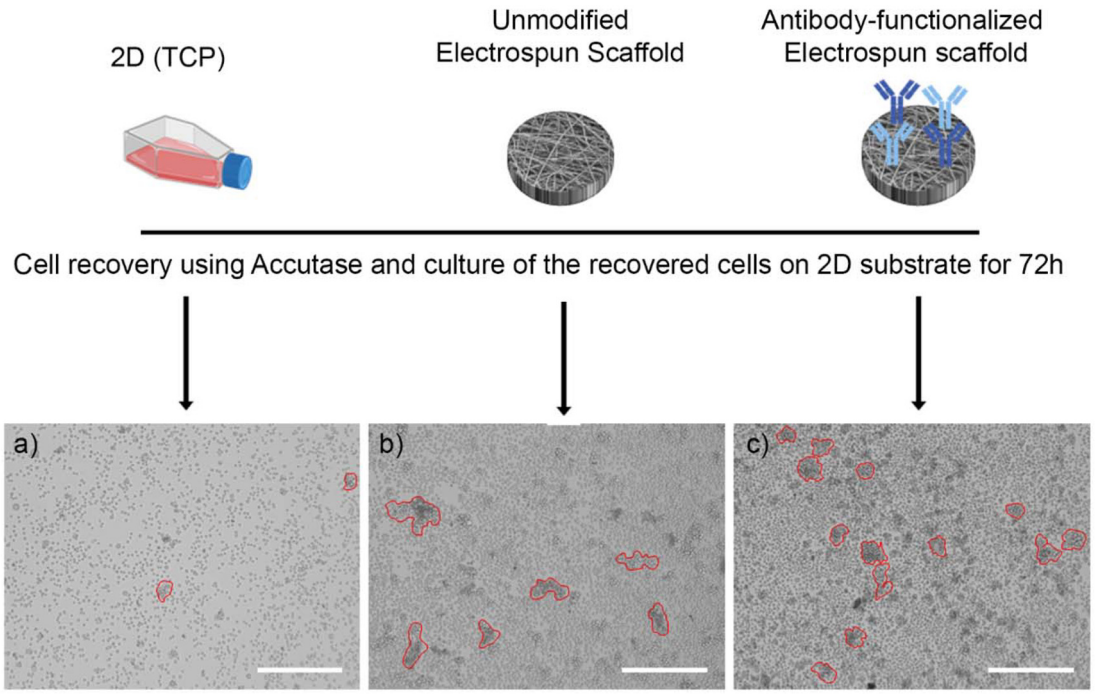

Fig. 5 Brightfield microscopy images showing the clustering ability of Jurkat cells (after 3 Days of culture in a 24-well non-tissue culture treated plate) recovered using Accutase from (a) 2D, (b) unmodified electrospun scaffold and (c) antibody-coated electrospun scaffold. Cell clusters are marked with red boundaries in the brightfield images. Scale: 300 μm.

ing methods from these fibrous scaffolds for retrieval of cells is inadequate.

In this study, Jurkat cells were cultured on Espun scaffolds and cell recovery methods were compared. The basal architecture offered by an electrospun scaffold is similar to the biological template of secondary lymphoid organs and is conducive to Jurkat cell attachment, retention and cellular ingrowth. This is determined not only by the pore size of scaffolds but also likely by their composition, thickness and mechanical properties. Earlier studies with softer PCL-PDMS blended fibres showed that these fibres can restore the proliferative capacity of the exhausted cell phenotype from patient samples.[5] However, the structural platform developed here using PCL offers a much simpler approach for scaffold fabrication compared to other fibrous scaffold systems. Surprisingly, these scaffolds could easily retain biomolecules on their surface through physical adsorption without additional functionalization. Further, we found out that even the suspension cells grown on these scaffolds could not be easily and adequately retrieved with gentle flushing using pipettes, as described by Dang *et al.*[5] The cells actively engage and interact with the scaffold fibres, making removal challenging through minimal application of force as described above. The strong interaction between cells and scaffolds suggests an affinity of T-cells towards the scaffold material, making it difficult to retrieve them.

The cell recovery methods primarily mentioned in the literature are either enzymatic cell dissociation methods (*viz.* Trypsin and Accutase), non-enzymatic using calcium ion chelating agents (*e.g.* EDTA), or manual flushing methods.[5,19,27–29] In our studies, we compared cell recovery using Accutase, Trypsin, and manual flushing. This study addresses a critical gap in the literature with respect to the efficiency of recovery of suspension cells from 3D scaffolds using these cell recovery methods. Each method of recovery has its own advantages and disadvantages. Cell surface receptors are often susceptible to enzymatic cleavage, and prior studies have identified inconsistencies in receptor cleavage when using Accutase.[17,28] Since T-cell activation requires extracellular stimulatory signals that are mediated by T cell receptor (TCR) complexes, the receptor cleavage resulting from any of the cell recovery strategies needs to be minimized. Trypsin-based cell recovery is known to increase receptor cleavage from cells.[29] A comparative assessment across all recovery methods tested in this study showed that cell recovery was similar and that there was no significant improvement in the cell yield from the scaffolds using any one strategy. Moreover, complete cell recovery from scaffolds was impossible due to the complex mesh-like network and strong interaction of the cells with scaffold fibres. Previous studies have suggested that factors such as pore size, fibre diameter, and scaffold material can influence the ease of cell retrieval.[30] Tightly packed fibres enhance cell attachment compared to loosely packed electrospun fibres. Consequently, their removal is dependent upon the extent of points of interaction between cells and enzymatic solution in tightly packed fibres.[30]

The strong interaction observed between the cells and the fibrous matrix indicates that the synthetic scaffold used here is highly biocompatible and can serve as an effective *ex vivo* culture platform. Moreover, the interaction becomes stronger with the introduction of activating antibodies, which also amplifies the difficulty of removing the cells from the scaffolds. This makes the choice of recovery method even more critical as the nature of recovery solution might impact cell health. The duration of interaction of cells with the recovery agent also impacts cell health, which requires to be optimized. In this study, the exposure was limited to 5 minutes, which is considered safe for suspension and loosely adherent cells. This choice reflects our intention to use the shortest exposure time possible. Furthermore, to the best of our knowledge, there is no published literature specifically examining the sensitivity of T cells to enzymatic treatments with Accutase and TrypLE. Most studies that mention these treatments do not focus on T cell sensitivity but rather on monocytes, macrophages and cancer cells.[27,31,32] A time gradient for enzymatic exposure was also not pursued, as our preliminary microscopy-based assessments indicated a decline in cell viability when the exposure exceeded 10 minutes for both Jurkat cells and primary mouse splenocytes. Previous studies have similarly reported reduced viability in adherent cells following 10 minutes of enzymatic treatment.[29] While a 10-minute exposure appears suitable for certain cell types such as monocytes and macrophage,[27] even strongly adherent cells like mesenchymal stromal cells and sensitive stem cells have been effectively detached with as little as 5 minutes of TrypLE treatment.[28] Based on these findings and our own observations, we selected a 5-minute enzymatic exposure period for Jurkat cells to optimize cell recovery while preserving viability. However, none of the recovery methods achieved complete retrieval of cells from the antibody-coated groups. The percentage of cell recovery from the non-functionalized scaffolds is about twice compared to that from the antibody-functionalised matrices. However, our preliminary studies also show that the antibody-coated substrates offer better-activation stimulus compared to the antibody-coated 2D plates (data not shown). Thus, removing maximum number of cells from these substrates is critical to utilizing and integrating this platform in an ACT modality.

The viability of recovered cells is another crucial criterion that needs to be considered before reinfusing them into the patient as it determines their subsequent therapeutic effect. In our studies, we found that cell viability was similar across all recovery methods within the coated and uncoated groups of substrates. However, cell viability does decrease across all recovery methods when recovering cells from an antibody-functionalized substrate. This observation may be attributed to activation-induced cell death[33,34] wherein overstimulation could drive the cells towards an exhausted phenotype, eventually leading to cell death. However, this requires further exploration.

A critical requirement for effective adoptive immunotherapy is that the functionality of recovered cells must remain intact after the recovery process. In our study, we observed that the recovered cells were capable of proliferating on a 2D substrate after being detached from both antibody-functionalized and non-functionalized substrates, indicating that the cells remained healthy and viable. Despite the challenges associated with the initial recovery process, we observed that the cells recovered using Accutase were able to cluster together, which is a characteristic behaviour of proliferating T-cells, and that they underwent more population doublings compared to the other test groups. This suggests that the cells maintained their competence even after the enzymatic detachment process and that Accutase may be used as a preferred method of cell retrieval.

The superiority of Accutase over TrypLE method can be attributed to the compositional variation. Accutase is a proprietary mixture of proteolytic and collagenolytic enzymes derived from invertebrates and is known for its ability to gently dissociate cells by targeting both cell–cell and cell–extracellular matrix (ECM) interactions. Unlike TrypLE, which is a recombinant trypsin-like serine protease, Accutase exhibits broader enzymatic activity, including degradation of ECM components such as fibronectin, laminin, and collagen. This broader substrate specificity enhances its efficiency in releasing cells from complex substrates or 3D scaffolds without compromising cell viability or surface markers. Several studies have demonstrated that Accutase provides superior cell recovery and preserves membrane integrity and antigenicity better than TrypLE or trypsin, especially for sensitive cell types or primary cultures.[27,31,32] For example, Lai, Ting-Yu *et al.* (2022) demonstrated the effectiveness of Accutase as a cell recovery agent over non-enzymatic EDTA to safely detach adherent cells without compromising cell viability. Further, majority of cell surface receptors of murine macrophage cell line RAW264.7 remain intact after Accutase treatment.[27] This suggests that the compositional difference between Accutase and TrypLE may be responsible for effective cell recovery. To our knowledge we are the first to report on the recovery of T-cells using Accutase from Espun scaffolds, highlighting their potential applications in immunotherapy.

Throughout this study Jurkat cells were chosen as a model due to their robustness and ease of handling. However, the study leaves a scope for further validation using primary murine splenocytes, a more physiologically relevant and sensitive immune population. Existing literature supports the gentle dissociation properties of Accutase in preserving surface antigens on macrophages[27,31,32] and viability of cancer cells.[29] On the other hand, TrypLE has been utilized for harvesting primary MSCs in certain tissue dissociation workflows from standard cell culture substrates,[28] although its application for detaching T cells from 3D scaffolds remains largely unexplored. From a manufacturing perspective, the scalability of enzymatic methods, especially with Accutase, is advantageous. Accutase allows for reproducible, high-efficiency recovery with minimal manual handling, reducing operator variability and processing time1. While enzymatic reagents may have a higher cost compared to mechanical methods, their superior yield and consistency make them suitable for

large-scale adoptive cell therapy (ACT) pipelines, where quality and reproducibility are critical. Furthermore, efficient detachment reduces processing time and downstream losses, aligning well with Good Manufacturing Practice (GMP) standards in ACT workflows.

5 Conclusions

In conclusion, this study systematically evaluated the *ex vivo* culture of Jurkat cells on a synthetic electrospun substrate, previously identified as a potential T-cell stimulator. A critical challenge in T-cell culture is ensuring the recovery of functionally robust T-cells for downstream applications. To address this, various cell recovery methods, including commercially available dissociation agents and a manual flushing technique, were compared to optimize the detachment of cells from the scaffolds. Our findings indicated that all recovery methods achieved comparable overall cell yields, which is encouraging. Cells harvested using Accutase exhibited superior viability, quality, and functionality. This was evident by their enhanced proliferative capacity, tendency for cluster formation, and cell spreading compared to other methods. These characteristics are essential for therapeutic applications of these cells, where maintaining the functionality of recovered T-cells is paramount. Based on these results, we conclude that Accutase is the optimal cell dissociation agent for recovering functional T-cells from electrospun PCL scaffolds, offering an effective approach for advancing therapeutic and other downstream applications involving *ex vivo* cultured T-cells.

Author contributions

The study was conceptualized by PT, NC and JD; JD designed the experiments, carried out scaffold fabrication, performed the experiments, and analysed the data in consultation with PT and NC. JD handled the software and visualization aspects. PT and NC supervised the study. JD wrote the initial draft. NC and PT jointly performed the review and editing. All authors discussed the results and commented on the manuscript.

Conflicts of interest

There are no conflicts to declare.

Data availability

The raw files for various microscopy images (SEM, fluorescence, confocal, and brightfield), flow plots, and cell viability data (Trypan blue cell counts) for this article are accessible at Monash University Bridges *via* the following **https://doi.org/10.26180/29276096**.

Supplementary information is available. Data information that are provided in the supplementary includes, (1) A table showing the optimization of the electrospun fibre synthesis, (2) SEM Images of the electrospun scaffolds, (3) Schematics showing the different cell recovery methods used and the viability comparison post recovery, (4) Graphs showing % of cells showing CFSE fluorescence Signal post recovery from the antibody coated Espun scaffold on Day 3 and Day 7, (5) Box and whisker plots depicting the cell spread area and circularity, (6) Stitched images of calcein stained Jurkat cells recovered from stimulating 2D and Espun substrates, (7) Fluorescence microscopy images for Live/Dead assay analysis of recovered Jurkat cells from the antibody coated Espun scaffolds, (8) Flow cytometry plots showing the gating strategy of CFSE stained Jurkat cells to determine extent of cell proliferation and (9) Bar graph showing the viability comparison between the various cell recovery methods, post recovery from antibody coated and uncoated substrates. See DOI: **https://doi.org/10.1039/d5bm00877h**.

Acknowledgements

We thank the Department of Biotechnology (DBT, Govt. of India), grant number- BT/NBDB/12/03/2016 and Monash University for the financial support. P. T. acknowledges funding from Department of Health Research – Indian Council of Medical Research grant number R.11017/21/2023-GIA/HR. N. R. C. acknowledges funding from the Australian Research Council for the Industrial Transformation Training Centre for Cell and Tissue Engineering Technologies (CTET), grant number- IC190100026. The European Union is gratefully acknowledged for funding through the project SURE-Poly (Marie Skłodowska-Curie grant agreement No. 101085759). We are thankful to the IITB-Monash Research Academy, Department of Biosciences and Bioengineering (BSBE), Indian Institute of Technology Bombay (IITB) and Department of Materials Science and Engineering (MSE), Monash University for providing the research infrastructure and facilities. Additionally, we would like to thank Dr Hemavathi Dhandapani (Post-doctoral research scholar, Cell and Tissue Engineering Lab) IITB, Dr Hiren Dandia, Haimanti Mukherjee and Shivali Patkar (Cell and Tissue Engineering Lab, IITB), Ms. Saranya Ajesh, (Project staff, BSBE, IITB), Dr Jennifer Dyson (Senior PC2 Lab manager, Monash University) and Mr Brendan Hung (Assistant PC2 Lab Manager, Monash University), Mr Jeremy Oon, Mr Sadjad Khoravimelal, MSE, Monash University for their help and support.

References

1 S. Han and J. Wu, *Bioact. Mater.*, 2022, **17**, 300–319.
2 Y.-H. Kim, S. Vijayavenkataraman and G. Cidonio, *BMC Med.*, 2024, **1**, 2.
3 I. Jun, H.-S. Han, J. R. Edwards and H. Jeon, *Int. J. Mol. Sci.*, 2018, **19**, 745.

4 A. Cipitria, A. Skelton, T. R. Dargaville, P. D. Dalton and D. W. Hutmacher, *J. Mater. Chem.*, 2011, **21**, 9419–9453.
5 A. Dang, S. De Leo, D. R. Bogdanowicz, D. J. Yuan, S. M. Fernandes, J. R. Brown, H. H. Lu and L. C. Kam, *Adv. Biosyst.*, 2018, **2**(2), 1700167.
6 H. S. Kim, T. C. Ho, M. J. Willner, M. W. Becker, H. W. Kim and K. W. Leong, *Bioact. Mater.*, 2023, **21**, 241–252.
7 Z. Safari, M. Sadeghizadeh, A. Zavaran Hosseini, A. Hazrati and S. Soudi, *Biomed. Pharmacother.*, 2024, **173**, 116382.
8 Y. Li, J. Wang, D. Qian, L. Chen, X. Mo, L. Wang, Y. Wang and W. Cui, *J. Nanobiotechnol.*, 2021, **19**, 131.
9 D. Venugopal, S. Vishwakarma, I. Kaur and S. Samavedi, *Acta Biomater.*, 2023, **163**, 228–247.
10 W. Jin, F. Tamzalit, P. K. Chaudhuri, C. T. Black, M. Huse and L. C. Kam, *Proc. Natl. Acad. Sci. U. S. A.*, 2019, **116**, 19835–19840.
11 J. Hu, A. A. Gondarenko, A. P. Dang, K. T. Bashour, R. S. O'Connor, S. Lee, A. Liapis, S. Ghassemi, M. C. Milone, M. P. Sheetz, M. L. Dustin, L. C. Kam and J. C. Hone, *Nano Lett.*, 2016, **16**, 2198–2204.
12 Z. Lokmic, T. Lämmermann, M. Sixt, S. Cardell, R. Hallmann and L. Sorokin, *Semin. Immunol.*, 2008, **20**, 4–13.
13 A. S. Cheung, D. K. Y. Zhang, S. T. Koshy and D. J. Mooney, *Nat. Biotechnol.*, 2018, **36**, 160–169.
14 T. Yang, J. Peng, Z. Shu, P. K. Sekar, S. Li and D. Gao, *Micromachines*, 2019, **10**(12), 832.
15 K. Garg, N. A. Pullen, C. A. Oskeritzian, J. J. Ryan and G. L. Bowlin, *Biomaterials*, 2013, **34**, 4439–4451.
16 C. Sachar and L. Kam, *Front. Immunol.*, 2021, **12**, 14–23.
17 D. L. Harrison, Y. Fang and J. Huang, *Front. Phys.*, 2019, **7**(45), 321–338.
18 X. Zhang, T.-H. Kim, T. J. Thauland, H. Li, F. S. Majedi, C. Ly, Z. Gu, M. J. Butte, A. C. Rowat and S. Li, *Curr. Opin. Biotechnol.*, 2020, **66**, 236–245.
19 S. Chen, E. C. So, S. E. Strome and X. Zhang, *J. Immunol. Methods*, 2015, **426**, 56–61.
20 D. R. Green, N. Droin and M. Pinkoski, *Immunol. Rev.*, 2003, **193**, 70–81.
21 R. Arakaki, A. Yamada, Y. Kudo, Y. Hayashi and N. Ishimaru, *Crit. Rev. Immunol.*, 2014, **34**, 301–314.
22 W. K. Wong, B. Yin, A. Rakhmatullina, J. Zhou and S. H. D. Wong, *Eng. Regener.*, 2021, **2**, 70–81.
23 A. Isser, N. K. Livingston and J. P. Schneck, *Biomaterials*, 2021, **268**, 120584.
24 Z. Zhang, Q. Liu, J. Tan, X. Zhan, T. Liu, Y. Wang, G. Lu, M. Wu and Y. Zhang, *Acta Pharm. Sin. B*, 2021, **11**, 1965–1977.
25 M. H. W. Chin, M. D. A. Norman, E. Gentleman, M.-O. Coppens and R. M. Day, *ACS Appl. Mater. Interfaces*, 2020, **12**, 47355–47367.
26 A. Wahl, C. Dinet, P. Dillard, A. Nassereddine, P.-H. Puech, L. Limozin and K. Sengupta, *Proc. Natl. Acad. Sci. U. S. A.*, 2019, **116**, 5908–5913.
27 T.-Y. Lai, J. Cao, P. Ou-Yang, C.-Y. Tsai, C.-W. Lin, C.-C. Chen, M.-K. Tsai and C.-Y. Lee, *Sci. Rep.*, 2022, **12**, 5713.
28 K. Tsuji, M. Ojima, K. Otabe, M. Horie, H. Koga, I. Sekiya and T. Muneta, *Cell Transplant.*, 2017, **26**, 1089–1102.
29 A. Nowak-Terpiłowska, P. Śledziński and J. Zeyland, *Braz. J. Med. Biol. Res.*, 2021, **54**, e10197.
30 F. F. R. Damanik, G. Spadolini, J. Rotmans, S. Farè and L. Moroni, *Biomater. Sci.*, 2019, **7**, 1088–1100.
31 Q. Song, Y. Zhang, M. Zhou, Y. Xu, Q. Zhang, L. Wu, S. Liu, M. Zhang, L. Zhang, Z. Wu, W. Peng, X. Liu and C. Zhao, *Front. Immunol.*, 2022, **13**, 920232.
32 N. Feuerer, J. Morschl, R. Daum, M. Weiss, S. Hinderer, K. Schenke-Layland and C. Shipp, *J. Immunol. Regener. Med.*, 2021, **11**, 100035.
33 D. R. Green, N. Droin and M. Pinkoski, *Immunol. Rev.*, 2003, **193**, 70–81.
34 R. Arakaki, A. Yamada, Y. Kudo, Y. Hayashi and N. Ishimaru, *Crit. Rev. Immunol.*, 2014, **34**, 301–314.

